

Characterization of deep levels in 6H-SiC by optical-capacitance-transient spectroscopy

Y. Nakakura, M. Kato,^{a)} M. Ichimura, and E. Arai

Department of Electrical and Computer Engineering, Nagoya Institute of Technology, Gokiso, Showa, Nagoya 466-8555, Japan

Y. Tokuda

Department of Electronics, Aichi Institute of Technology, Yakusa, Toyota 470-0392, Japan

S. Nishino

Department of Electronics and Information Science, Kyoto Institute of Technology, Matsugasaki, Sakyo, Kyoto 606-8585, Japan

(Received 1 April 2003; accepted 19 June 2003)

An optical-capacitance-transient spectroscopy (O-CTS) method was used to characterize defects in epitaxial 6H-SiC. The O-CTS measurements enable us to estimate the optical ionization energy and the optical cross section of these defects. By the deep level transient spectroscopy (DLTS), three peaks were observed, and two of them were identified as *E2* and *R* centers which have been previously reported. We measured the optical cross section for both the centers. By fitting the experimental data with theoretical curves for the optical cross section, we obtained optical ionization energy of 1.58 eV for the *R* center and 1.0 eV for the *E2* center. From the DLTS measurements, the thermal activation energy of the *R* center is 1.30 eV and that of the *E2* center is 0.43 eV. From these results and the previously reported capture energy barrier, the Franck-Condon shift, d_{FC} is estimated to be 0.28 eV for the *R* center and 0.62 eV for the *E2* center. © 2003 American Institute of Physics. [DOI: 10.1063/1.1600528]

I. INTRODUCTION

Silicon carbide (SiC) is a promising material for high-temperature, high-power and high-frequency electronic devices because of its wide band gap, high thermal conductivity and high electron saturation velocity. In recent years, high-quality epitaxial layers were able to be grown by the chemical vapor deposition (CVD) method.¹ However a considerable density of defects is still present in the epitaxial layers, and these defects may introduce deep levels into the band gap. These deep levels act as a recombination center or an electron (hole) trap, and consequently they affect device performance. So far, these deep levels have been investigated by deep level transient spectroscopy (DLTS),² photoluminescence (PL),³ electron spin resonance (ESR)⁴ and so on, but the nature of those deep levels has not been fully characterized.

In this article, we report on characterization of the deep levels in *n*-type epitaxial 6H-SiC by optical-capacitance-transient spectroscopy (O-CTS),^{5,6} which enables us to measure the optical transition rate of electrons from the deep levels to the conduction band. One advantage of this method is that heating of the sample to high temperature is not required even for the measurement of midgap levels in contrast to the DLTS. We compare the optical ionization energy with the thermal activation energy and discuss the interaction between electrons and the lattice.

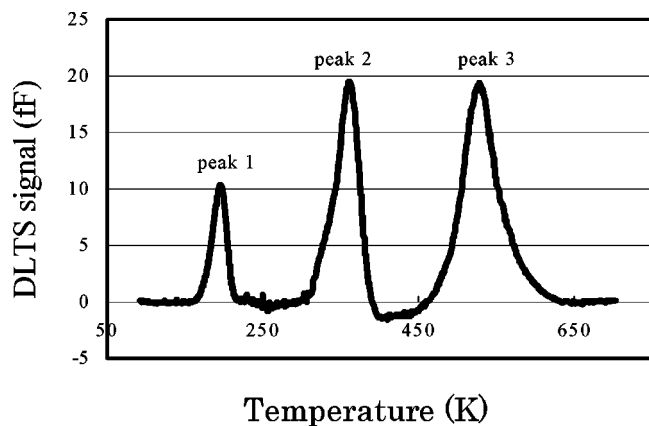
II. EXPERIMENT

The sample used in this work was an *n*-type 6H-SiC grown on a 6H-SiC (0001) Si face substrate inclined at 3.5° toward $\langle 11\bar{2}0 \rangle$ by the cold wall CVD method in atmospheric pressure. Source gases were Si₂Cl₆ and C₃H₈ with a H₂ carrier gas, and the growth temperature was 1550 °C.⁷ The Si/C ratio for source gases was approximately 0.1. This sample is the same as that characterized by DLTS in Ref. 8.

After growth, Ni was evaporated onto the C face of the sample and it was annealed at 1150 °C in order to form ohmic contact. Au was evaporated onto the epitaxial layer surface as a Schottky contact. The Au contact is thin enough (~ 50 nm) to be transparent for excitation light, and is of 1 mm² area. By using these contacts, capacitance-voltage (*C-V*), DLTS, capacitance transient spectroscopy (CTS) and O-CTS measurements were performed. The DLTS, CTS and O-CTS measurements were done with reverse bias of -4.0 V and injection bias of 0 V.

In the CTS measurement, we detected a capacitance transient signal caused by the excitation of carriers from deep levels at constant temperature. The signal was converted to the CTS spectrum by using the rate window scan method with a bipolar rectangular weighting function.⁹ O-CTS measurement is almost the same as CTS measurement except that carriers are excited by light. At temperatures at which the thermal excitation of the carriers from the deep levels is negligible, the time constant of the transient signal is given by $\tau = 1/\Phi\sigma^o$, where Φ is photon flux and σ^o is the optical cross section. In the O-CTS measurements, a 300 W xenon lamp was employed as a light source. The

^{a)}Electronic mail: mkato@hermite.elcom.nitech.ac.jp

FIG. 1. DLTS spectrum of 6H-SiC ($\tau=76$ ms).

monochromator output was focused onto the Schottky contact region. The energy range of the monochromatic light was 0.73–1.88 eV, and the lamp power was adjusted to give a constant photon flux for a series of spectra. Depending on the light source emission spectrum, two different levels of photon flux were employed, one was $5 \times 10^{15} \text{ cm}^{-2} \text{ s}^{-1}$ for 0.73–1.38 eV and the other was $1 \times 10^{16} \text{ cm}^{-2} \text{ s}^{-1}$ for 1.13–1.88 eV.

III. RESULTS

From the C - V measurement we obtain a net donor concentration of 6H-SiC of $4 \times 10^{15} \text{ cm}^{-3}$. Figure 1 shows the DLTS spectrum of the 6H-SiC with time constant of 76 ms, in which we observe three peaks. Peak 1 is similar to the $E1/E2$ center signal reported in Refs. 2, 10 and 11. The $E1/E2$ center is in fact two different centers ($E1$ and $E2$), and they are frequently observed as an apparently single DLTS peak because of overlapping of the two peaks. In order to see this overlapping in peak 1, we performed CTS measurements, with which it is easier to separate the peaks than by DLTS measurements. This peak seems to correspond to a single defect level, and its activation energy is 0.43 eV, which is closer to the activation energy of the $E2$ center rather than to the $E1$ center.¹⁰ Thus peak 1 is attributed to the $E2$ center. Peak 2, observed around 350 K, has an activation energy of 0.79 eV, but we will show later that this peak consists of more than two peaks with almost the same activation energy. Peak 3, observed around 550 K, looks like a single peak. However we found that peak 3 is also the overlap of two peaks as shown in Fig. 2 using CTS measurements. Peaks 3a and 3b are caused by defects with activation energies of 1.30 and 1.54 eV, respectively. The activation energy for peak 3a is close to that of the R center, which has been reported by Dalibor *et al.*² Therefore peak 3a is caused by the R center.

Figure 3 shows O-CTS spectra at a measurement temperature of 370 K for 1.13–1.88 eV photon energies. At this temperature, the thermal excitation rate from the $E2$ center is much higher than the observation time window, thus we can neglect the influence of the $E2$ center. Without illumination, only one peak was observed around a time constant of 0.1 s. Because the time constant of this peak did not change with

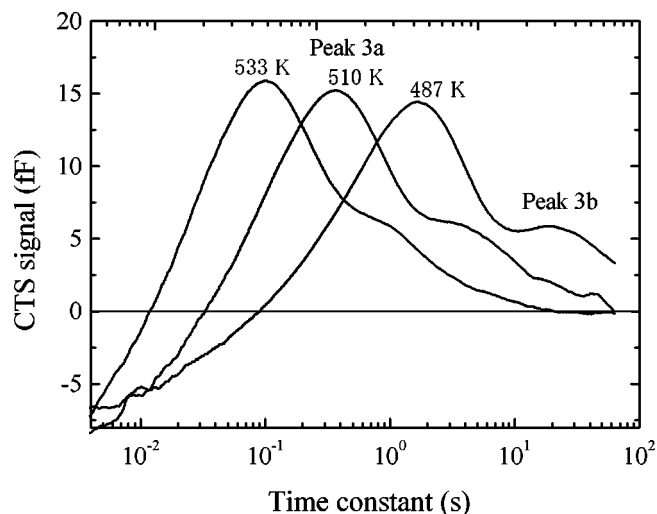
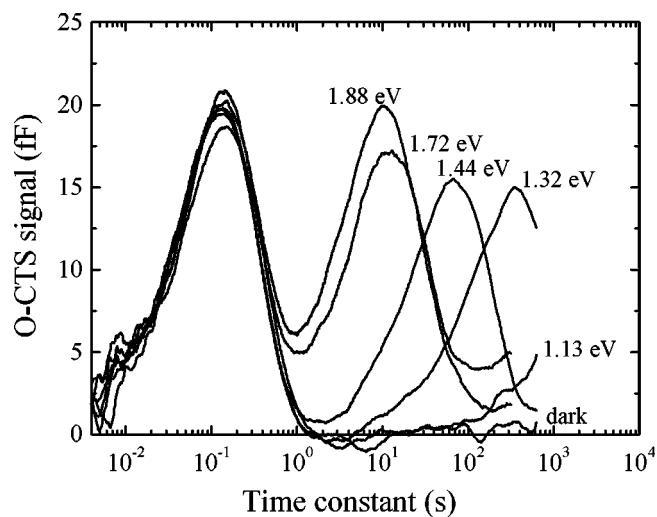


FIG. 2. CTS spectra at 487–533 K.

illumination, this peak was caused by thermal excitation that corresponds to peak 2 in the DLTS spectrum. With 1.13 eV illumination, the shoulder of another peak appeared at a time constant of 10^2 – 10^3 s. With an increase in photon energy, the time constant of the peak decreased. This peak has almost the same height as peak 3a (R center) observed in the CTS spectra (Fig. 2). Thus the peak observed in the O-CTS spectra with 1.13–1.44 eV illumination is identical to the peak originating from the R center. For more than 1.72 eV illumination, the peak height increased with an increase in photon energy. This is because of overlapping with another peak, probably the peak 3b. The time constant of the peak did not change significantly in this energy range (>1.72 eV). From these results, we plot the optical cross section for the R center in Fig. 4. The optical cross section of the R center increases with an increase in photon energy and it tends to saturate above 1.7 eV. These data are fitted by a theoretical model proposed by Chantre *et al.*¹² In this model, the impurity potential is represented by a Dirac well, and the

FIG. 3. O-CTS spectra with 1.13–1.88 eV illumination at 370 K. (The photon flux is $6 \times 10^{15} \text{ cm}^{-2} \text{ s}^{-1}$.)

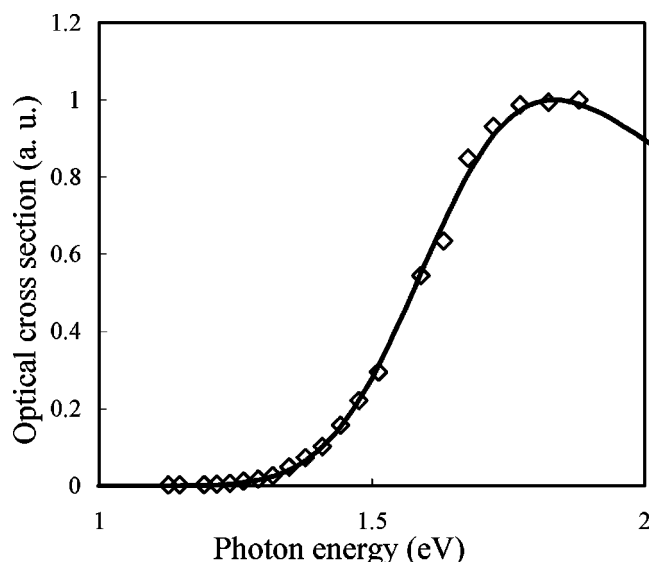


FIG. 4. Optical cross section of peak 3a (the *R* center). The solid line represents the theoretical curve.

bound state wave function is given by the effective mass approximation,

$$\Psi_T(r) \propto (1/r) \exp(-\alpha r), \quad (1)$$

where r is the distance from the trap and α^{-1} is a fitting parameter. The mathematical formula for σ^o used in this model is^{6,12}

$$\sigma^o \propto \frac{1}{y \theta^{1/2}} \int_1^\infty \frac{(x-1)^{1/2}}{(x-1 + E^i/E^o)^2} \exp\left[-\frac{(y-x)^2}{\theta}\right] dx, \quad (2)$$

$$\theta = \frac{4d_{FC}kT}{E^o{}^2}, \quad y = \frac{h\nu}{E^o}, \quad \text{and} \quad E^i = \frac{\hbar^2 \alpha^2}{2m^*},$$

where E^o , d_{FC} and m^* are the optical ionization energy, the Franck–Condon energy, which indicates the strength of the electron–lattice interaction, and the effective mass of the electron, respectively. In the curve fitting calculation, the effective mass of the electron = $0.69m_o$.¹³ We have a good fit between the theoretical and experimental data curves when $E^o = 1.58$ eV and $\alpha^{-1} = 3$ Å. The capture energy barrier of the *R* center has been reported to be negligible,¹⁰ and therefore its Franck–Condon energy $d_{FC} = 0.28$ eV.

Figure 5 shows O-CTS spectra at 130 K with photon energies ranging from 0.73 to 1.38 eV. Without illumination, no peak was observed within the measurement time constant. With 0.73 eV illumination, a peak was observed around a time constant of 300 s. This peak was broader than the theoretical curve. With 1.09 eV illumination, two peaks, which are partly overlapped, were observed. The optical ionization energies of these peaks are lower than that of the *R* center because, with less than 1.13 eV illumination, the peak caused by the *R* center was not observed within the measurement time constant as shown in Fig. 3. In the DLTS spectrum, the peaks with activation energy lower than that of the *R* center are only peak 1 and peak 2. Therefore the two peaks in the O-CTS spectra (Fig. 5) correspond to peak 1 (the *E2* center)

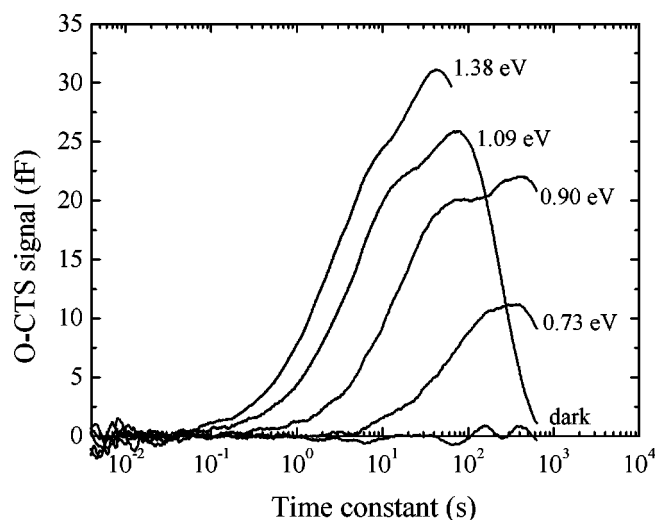


FIG. 5. O-CTS spectra with 0.73–1.38 eV illumination at 130 K. (The photon flux is $2 \times 10^{15} \text{ cm}^{-2} \text{ s}^{-1}$.)

and peak 2 in the DLTS spectrum. With 1.38 eV illumination, the peak height increased further because the peak for the *R* center overlaps these two peaks.

Figure 6 shows O-CTS spectra at 220 K with 0.73–1.38 eV photon energies. The peak around 0.02 s is caused by the *E2* center (peak 1 in the DLTS spectrum). The time constant of this peak did not change with illumination, and thus this peak originates from thermal excitation. With 0.73 eV illumination, the shoulder of the peak appeared at a time constant of about 10^3 s. With an increase in photon energy, the time constant of this peak became smaller. With 1.09 eV illumination, the peak time constant decreased to about 10^2 s. With more than 0.90 eV illumination, however, the peak was broader than the theoretical curve, and thus it was the overlapping of more than two peaks. Taking the measurement temperature and the photon energy range into consideration, we expect that no peak should appear except for peak 2. Therefore this peak is identical to peak 2 in the DLTS

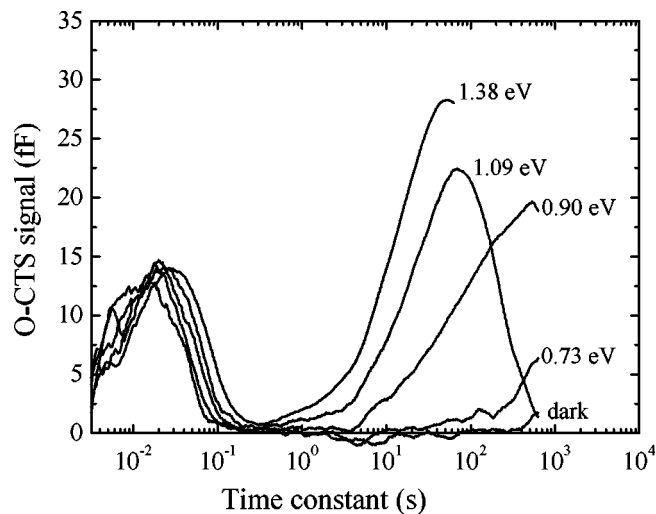


FIG. 6. O-CTS spectra with 0.73–1.38 eV illumination at 220 K. (The photon flux is $2 \times 10^{15} \text{ cm}^{-2} \text{ s}^{-1}$.)

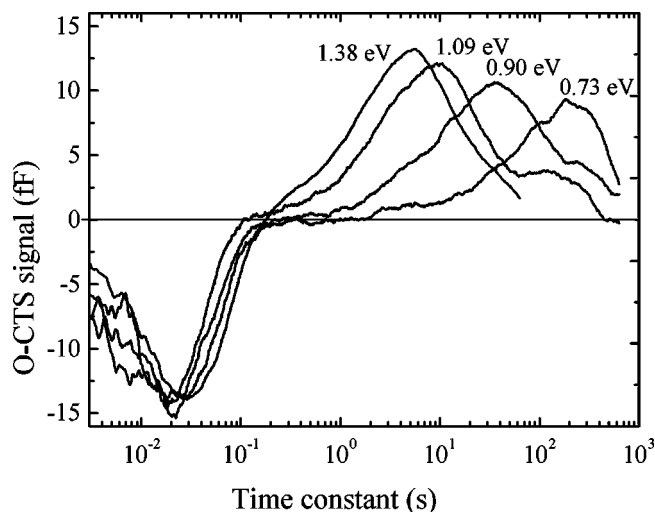


FIG. 7. O-CTS spectra obtained by subtraction of the spectra at 220 K from those at 130 K.

spectrum, and peak 2 is in fact overlapping of more than two peaks. This overlapping makes it impossible to estimate the optical cross section.

Figure 7 shows O-CTS spectra obtained from subtraction of the O-CTS spectra at 220 K (Fig. 6) from those at 130 K (Fig. 5) for observation of the *E2* center spectra. Considering the measurement temperature, the O-CTS peak in Fig. 5 is the overlapping of peak 1 (the *E2* center), peak 2 and peak 3a (the *R* center), while, in Fig. 6, the peak observed at a time constant of $10\text{--}10^3$ s overlaps peak 2 and peak 3a. Therefore, from subtraction of both O-CTS spectra, we can observe the O-CTS peak originating only from the *E2* center. The negative peaks observed at 2×10^{-2} s in all the spectra in Fig. 7 are caused by the subtraction procedure. With 0.73 eV illumination, the peak is observed at a time constant of about 2×10^2 s. With an increase in photon energy, this peak time constant decreases. The peak height increases with the photon energy, probably because of inaccuracy in the subtraction procedure. If the optical cross section of peak 2 depends on the temperature, both the shape and the height of the peak should be different between 180 and 220 K, and therefore we cannot accurately subtract the peak 2 signal from the 180 K spectra.

From the peak positions of the spectra in Fig. 7, the optical cross section of the *E2* center is plotted in Fig. 8. The theoretical curve best fits experimental data when $E^0 = 1.0$ eV and $\alpha^{-1} = 1.3$ Å. With photon energies of more than 1.4 eV, the optical cross section deviates from the theoretical curve. This may be due to excitation from the *E2* center to the second conduction band minimum, because the theoretical curve considers only one excitation process, which is excitation from a deep center to the conduction band minimum.

We searched for deeper levels by increasing the photon energy up to 2.48 eV, but we found no other peak. This does not mean that there are no other deep levels, because, in the O-CTS measurement with illumination of photon energy larger than half of the band gap energy (> 1.5 eV), a peak is not observed when the electron capture process from the va-

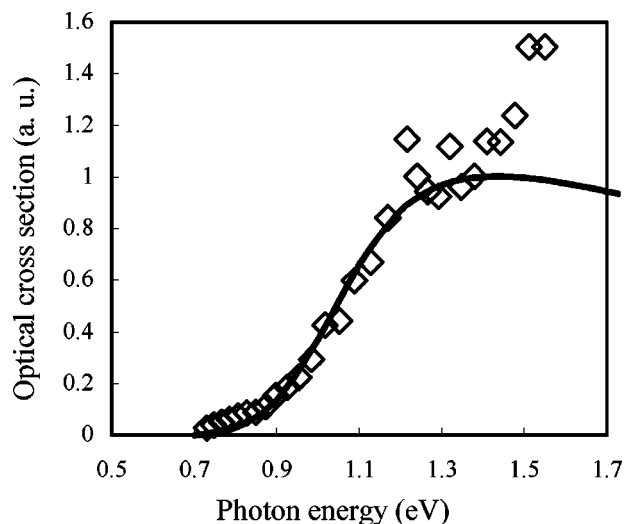


FIG. 8. Optical cross section of peak 1 (the *E2* center). The solid line represents the theoretical curve.

lence band dominates the emission process under illumination.

IV. DISCUSSION

The optical ionization energy and the thermal activation energy of the *R* center are 1.58 and 1.30 eV, respectively. The capture energy barrier of this center is negligibly small and this center is acceptor like.^{2,10} From these results a configuration coordinate diagram for the *R* center is obtained and is shown in Fig. 9.

Hemmingsson *et al.* have reported that the *E2* center has the negative-*U* property and has an acceptor state with an activation energy of 0.43 eV and a donor state with an activation energy of 0.27–0.29 eV.¹⁴ They have also reported that the capture process to an acceptor state is a multiphonon process with capture barrier of 0.05 eV, and that to a donor state is a cascade process.¹⁴ Taking these properties into ac-

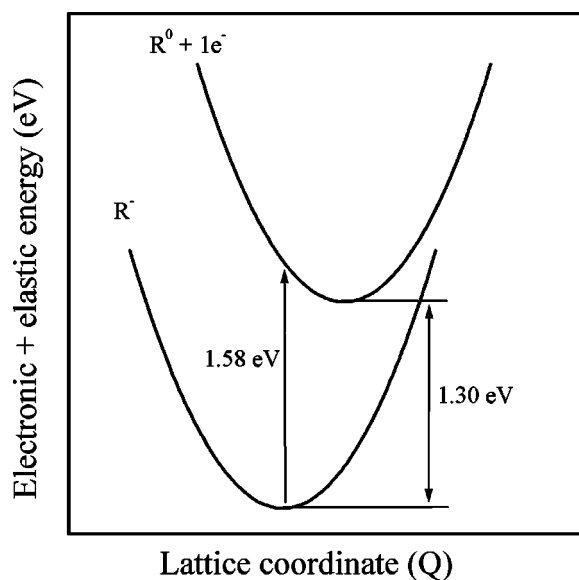
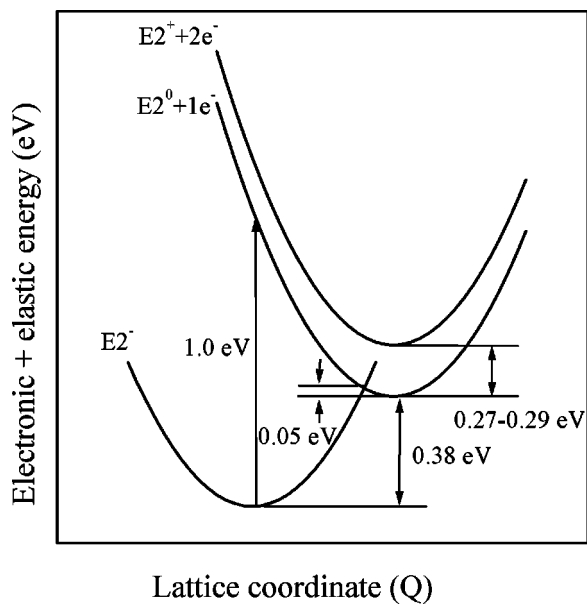


FIG. 9. Configuration coordinate diagram for the *R* center.

FIG. 10. Configuration coordinate diagram for the $E2$ center.

count, the configuration coordinate diagram for the $E2$ center is obtained and is shown in Fig. 10. For the acceptor state, the difference in energy between the minimum of the excited state branch and the cross point of the excited state branch with the ground state branch is 0.05 eV, corresponding to capture barrier of 0.05 eV. On the other hand, the difference in energy between that cross point and the minimum of the ground state branch is 0.43 eV, corresponding to thermal activation energy of 0.43 eV. Thus the energy level of the acceptor state of the $E2$ center is located at $E_c - 0.38$ eV. Since the optical ionization energy of this center is 1.0 eV, the difference in energy between the minimum of the ground state branch and the excited state branch at the same lattice coordinate is 1.0 eV. For the donor state, the capture process is a cascade process,¹⁴ and thus the electron–lattice interaction is weak. Therefore in Fig. 10, the difference in lattice coordinate between the excited state and the ground state (the excited state of the acceptor state) is assumed to be null, and the difference in energy between them is 0.27–0.29 eV. For the acceptor state, $d_{FC} = 0.62$ eV, and thus its electron–lattice interaction is very large. This large d_{FC} property is similar to the DX center in AlGaAs, which also has the negative- U property.¹⁵ In general, the negative- U center should have large d_{FC} in order to overcome electron repulsive energy around the center by gaining lattice relaxation energy.

Redmann *et al.*¹⁶ reported that the optical ionization energy of the $E1/E2$ center is 0.47 eV. However our result is 1.0 eV, which is different from theirs. They used positron annihilation spectroscopy (PAS) and observed the average positron lifetime change by varying the illumination photon energy. In this case, this lifetime is influenced not only by the $E1/E2$ center but also by other defects. They attributed the lifetime change by illumination to the $E1/E2$ center simply because the threshold photon energy (0.47 eV) is close to the thermal activation energy of the $E1/E2$ center (0.43 eV). This assignment is obviously inappropriate for a center with

large d_{FC} . We believe that they observed the optical ionization of some other defects.

Frank *et al.*¹⁷ have reported that the $E1/E2$ center observed in DLTS spectra and $D1$ center (L_1 , L_2 and L_3 lines) observed in low temperature photoluminescence (LTPL) spectra with 2.6 eV radiation energy are the same defect center. In LTPL spectra, the $D1$ center has an intense zero-phonon line and a weak one-phonon line (phonon replica).¹⁸ When the electron–lattice interaction is strong, i.e., d_{FC} is large, the phonon side band must be stronger than the zero-phonon line.¹⁹ Therefore the electron–lattice interaction of the $D1$ center is expected to be weak. As described above, d_{FC} of the donor state of the $E2$ center will be small because its capture process is cascade capture.¹⁴ On the other hand, the acceptor state has large d_{FC} , 0.62 eV. Therefore our results indicate that if the $D1$ center and the $E2$ center are identical defects, the PL peaks caused by the $D1$ center corresponds to the electron transition from the donor state of the $E2$ center to the valance band. The radiation energy of the $D1$ center is about 2.6 eV, which corresponds to the transition from the energy state of $E_c - 0.4$ eV, which is slightly different from the donor state, $E_c - (0.27 - 0.29)$ eV. This slight difference in energy may be due to the Poole–Frenkel effect. This effect means that the activation energy of a donor state is lowered by electric fields. Thus the donor state of the $E2$ center is influenced by this effect. In Ref. 14, estimation of the energy level of the donor state was performed with a DLTS measurement, in which an electric field is applied to deep levels in a junction depletion layer, whereas, in the LTPL measurement, no electric field is applied to deep levels.^{17,18} Thus, one can consider that the activation energy of the donor state at zero electric field is more than 0.27–0.29 eV, or near to 0.4 eV, which corresponds to the energy state of the $D1$ center. It should be noted that the energy levels of the acceptor state of the $E2$ center and of the R center are not influenced by the Poole–Frenkel effect, since they are acceptors. Therefore our evaluation of the energy levels is not affected by the Poole–Frenkel effect.

V. CONCLUSION

We performed O-CTS and DLTS measurements to characterize the deep levels in 6H-SiC. From the DLTS and the CTS measurements, four peaks were observed. The activation energy of peak 1 (the $E2$ center), peak 2, peak 3a (the R center) and peak 3b were found to be 0.43, 0.79, 1.30 and 1.54 eV, respectively. From the O-CTS measurements, the optical ionization energies of the $E2$ center and the R center are 1.0 and 1.58 eV, respectively. d_{FC} obtained from these results is 0.62 eV for the $E2$ center and 0.28 eV for the R center. Therefore the $E2$ center has the large electron–lattice interaction. We obtained the configuration coordinate diagram for the $E2$ center and the R center.

¹H. Matsunami and T. Kimoto, *Mater. Sci. Eng., R.* **20**, 125 (1997).

²T. Dalibor, G. Pensl, H. Matsunami, T. Kimoto, W. J. Choyke, A. Schöner, and N. Nordell, *Phys. Status Solidi A* **162**, 199 (1997).

³L. Patrick and W. J. Choyke, *Phys. Rev. B* **5**, 3253 (1972).

⁴V. S. Vainer and V. A. Il'in, *Sov. Phys. Solid State* **23**, 2126 (1981).

⁵Y. Nakakura, M. Kato, M. Ichimura, E. Arai, and Y. Tokuda, *Mater. Res. Soc. Symp. Proc.* **719**, 167 (2002).

- ⁶P. Hacke, H. Okushi, T. Kuroda, T. Detchprohm, K. Hiramatsu, and N. Sawaki, *J. Cryst. Growth* **189**, 541 (1998).
- ⁷Y. Masuda, S. Oshima, C. Jacob, and S. Nishino, *Mater. Sci. Forum* **353–356**, 139 (2001).
- ⁸M. Kato, M. Ichimura, E. Arai, and S. Nishino, *Mater. Res. Soc. Symp. Proc.* **719**, 457 (2002).
- ⁹Y. Tokuda, N. Shimizu, and A. Usami, *Jpn. J. Appl. Phys., Part 2* **18**, L309 (1979).
- ¹⁰C. G. Hemmingsson, N. T. Son, O. Kordina, and E. Janzen, *J. Appl. Phys.* **84**, 704 (1998).
- ¹¹M. Gong, S. Fang, C. D. Beling, and Z. You, *J. Appl. Phys.* **85**, 7604 (1999).
- ¹²A. Chantre, G. Vincent, and D. Bois, *Phys. Rev. B* **23**, 5335 (1981).
- ¹³C. Persson and U. Lindefelt, *J. Appl. Phys.* **82**, 5496 (1997).
- ¹⁴C. G. Hemmingsson, N. T. Son, and E. Janzen, *Appl. Phys. Lett.* **74**, 839 (1999).
- ¹⁵P. M. Mooney, *J. Appl. Phys.* **67**, R1 (1990).
- ¹⁶F. Redmann, A. Kawasuso, K. Petters, H. Itoh, and R. Krause-Rehberg, *Physica B* **308–310**, 629 (2001).
- ¹⁷T. Frank, G. Pensl, S. Bai, R. P. Devaty, and W. J. Choyke, *Mater. Sci. Forum* **338–342**, 753 (2000).
- ¹⁸A. Fissel, W. Richter, J. Furthmuller, and F. Bechstedt, *Appl. Phys. Lett.* **78**, 2521 (2001).
- ¹⁹J. Bourgoin and M. Lannoo, *Point Defects in Semiconductors II* (Springer, Berlin, 1983).